Experimental Studies of Pattern Formation in a Reaction-Advection-Diffusion System

C. R. Nugent, W. M. Quarles, and T. H. Solomon*

Department of Physics, Bucknell University, Lewisburg, Pennsylvania 17837, USA

(Received 20 May 2004; published 18 November 2004)

Experiments are presented on pattern formation in the Belousov-Zhabotinsky (BZ) reaction in a blinking vortex flow. Mixing in this flow is chaotic, with nearby tracers separating exponentially with time. The patterns that form in this flow with the BZ reaction mimic chaotic mixing structures seen in passive transport. The behavior is analyzed in terms of a mixing time τ_m and a characteristic decorrelation time T_{BZ} for the BZ system. Flows with τ_m comparable to or smaller than T_{BZ} generate large-scale patterns whose features are captured by simulations of mixing fields for the flow.

DOI: 10.1103/PhysRevLett.93.218301 PACS numbers: 82.40.Ck, 05.45.–a, 47.52.+j, 47.54.+r

There is a great deal of interest in understanding how patterns form in nonlinear dynamical systems. In particular, there have been numerous studies of *reaction-diffusion* problems [1,2], such as chemically reacting fluids [3,4], interacting populations and ecosystems [5], and systems with propagating fronts [6,7]. By definition, there are no flows in a reaction-diffusion system; any mixing between the different species is achieved solely via diffusion. In most real fluids, however, flows in the system significantly enhance mixing beyond that due to diffusion alone. This advective mixing has a significant influence on the pattern formation process. This is particularly important in light of recent studies that show that mixing can be chaotic even for simple, well-ordered laminar fluid flows [8,9]. Some recent theoretical and numerical studies have considered the influence of chaotic advection on chemical and biological pattern-forming systems [10–13]. In particular, the studies have shown that chaotic mixing in reacting systems typically produces filamentary patterns, with the filaments mimicking the structures used to describe chaotic mixing in the flows [14,15].

In this Letter, we present results of *experimental* studies of pattern formation in a *reaction-advection-diffusion* system: the Belousov-Zhabotinsky (BZ) reaction in a blinking vortex flow—a simple, laminar flow in which the mixing is chaotic. The BZ system initially attracted attention since the chemical reaction oscillates when well mixed. When confined to a thin, two-dimensional layer *without any flows*, the BZ chemicals spontaneously develop stripe and spiral patterns [16,17]. We investigate what happens to these patterns when the blinking vortex flow is present in the system. In particular, the reaction-advection-diffusion patterns that form are compared to the structures associated with chaotic mixing of impurities in this flow.

The blinking vortex flow [8] [Fig. 1(a)] can be described by the following set of equations:

$$\dot{x} = -\frac{Ay}{x_s^2 + y^2}, \qquad \dot{y} = \frac{Ax_s}{x_s^2 + y^2}, \tag{1}$$

where

$$x_s = \begin{cases} x + b, & 0 < t < T/2 \\ x - b, & T/2 < t < T \end{cases}. \tag{2}$$

This is a two-dimensional, laminar fluid flow in which fluid alternately circles around a left and a right point vortex. The blinking period T can be characterized nondimensionally by $\mu = AT/a^2$, where a is the radius of the entire system. The parameter μ can be thought of as the ratio between the blinking period and the circulation time for fluid elements near the edge of the system.

Experimentally, the flow is generated using a magnetohydrodynamic technique [18–20], as shown in Fig. 1(b). The system is predominately two dimensional; the flow is confined to a thin (0.20 cm) layer of water containing a small concentration of H_2SO_4 (0.006 M) that is needed to conduct an electrical current. Two electrodes near the middle of the flow are separated by $2b = 1.9$ cm and

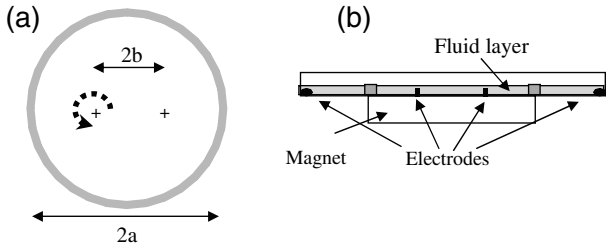

FIG. 1. (a) Top view of flow and (b) side view of apparatus for blinking vortex system. The flow alternates periodically between circulating around the left point vortex (labeled "+") as shown and circulating around the right vortex (not shown). The flow is forced magnetohydrodynamically: an electrical current enters the fluid through an outer ring electrode, then flows radially inward, converging on one of the two electrodes near the center. The interaction between this radial current and a strong magnetic field (produced by a 2.5 in. diameter Nd-Fe-B magnet) generates the vortical flow. The center electrodes are a distance of $2b = 1.9$ cm apart, and the region of interest (within the Plexiglas ring) has a diameter of $2a = 5.7$ cm and a thickness of 0.2 cm.

are surrounded by a bounding ring (inner diameter $2a = 5.7$ cm) and an outer electrode. The entire apparatus sits on a 2.5 in. diameter Nd-Fe-Bo magnet which produces a vertical magnetic field throughout the region of interest (within the bounding ring). During half of the blinking period, current flows radially between the left point electrode and the outer ring electrode. The radial current interacts with the magnetic field to produce a flow that circles around this electrode, as shown in Fig. 1(a). During the other half of the period, the current flows between the *right* point and outer electrodes, producing a flow that circles around that electrode.

Mixing in this flow is characterized by injecting a large blob of a neutrally buoyant impurity (0.103 μm fluorescent polystyrene microspheres with a diffusion coefficient of 4.5×10^{-8} cm^2/s) into the flow. The system is illuminated with black light, and images of the mixing are captured by a 12-bit charge-coupled device video camera. The resulting mixing is shown in Fig. 2. As is typical for chaotic systems, the mixing is characterized by repeated stretching and folding. A region of chaotic mixing occupies the middle of the flow [8]; the size of this chaotic region depends on the dimensionless blinking period μ. Throughout the remainder of this Letter, μ is held at 0.52, although the blinking frequency f and the vortex magnitude A are varied.

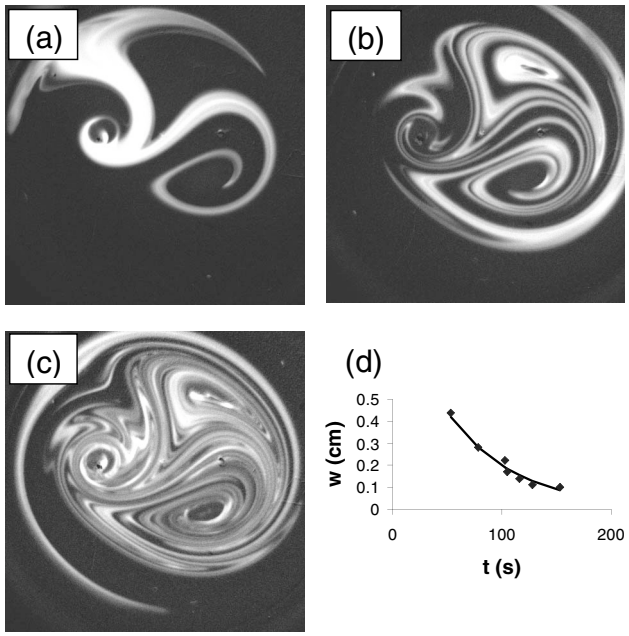

FIG. 2. Sequence showing the mixing of a passive tracer in the blinking vortex flow; period of blinking $T = 50s$; $\mu = 0.52$. Times after start are as follows: (a) 53 s (1 period); (b) 103 s (2 periods); (c) 203 s (4 periods). (d) Characteristic (ensemble average) filament width w for evolving dye distribution, determined experimentally by averaging the filament widths at numerous locations in each image. The smooth curve is a fit of the experimental data to a decaying exponential.

Given a particular value of μ, the mixing patterns due to advection are determined; mixing *times*, however, depend on more than just μ. Complete mixing occurs on a time scale determined by the interplay between advection and diffusion. The stretching and folding of chaotic advection reduces the typical thickness w of impurity filaments roughly exponentially in time, as shown in Fig. 2(d). The smooth curve is a fit $w(t) = w_0 e^{-\lambda t}$, with $\lambda = 0.79$ periods^{-1}. When the filament width w is sufficiently reduced, molecular diffusion, which mixes structures on a length scale $L_d \sim \sqrt{Dt}$, finishes the mixing. A mixing time scale τ_m, therefore, is then defined as the time that solves the implicit equation $w(t) = L_d(t)$. For w_0, we use the center-center vortex spacing 1.9 cm. For the diffusion coefficient D, we use a typical value for the chemicals in the BZ reaction ($D \simeq 1 \times 10^{-5}$ cm^2/s), since we are using the mixing time to analyze reaction-advection-diffusion patterns in the BZ system. An increase in the oscillation period T and a proportional decrease in the flow magnitude A maintain the same value of μ, but increases the mixing time τ_m, since it takes longer for each period of the blinking oscillation.

To study reaction-advection-diffusion patterns in this system, we replace the dilute H_2SO_4 by the chemicals used in the BZ reaction. (The solution is mixed from the following recipe: 40 ml of 1 M sulfuric acid, 1.144 g of malonic acid, 0.418 g of potassium bromate, 0.044 g of cerium ammonium nitrate, and 0.5 ml of 0.025 M ferroin.) The reaction oscillates between a red and a blue color. The system is illuminated with white light, and a blue filter is placed on the camera lens such that the red and blue phases show up as dark and light regions, respectively. The chemicals are initially well mixed, with the whole system oscillating red-blue uniformly. In the absence of any fluid flow, the uniform oscillations break up (within a couple hundred seconds) into a complex pattern of stripes, as seen in Fig. 3(a), typical of patterns usually seen in reaction-diffusion systems.

Figures 3(c)–3(e) show pattern formation in the same system with the blinking vortex flow turned on. All three cases have $\mu = 0.52$, but frequencies $f = 0.010$, 0.030, and 0.050 Hz, corresponding to mixing times $\tau_m = 400$, 160, and 100 s, respectively. For each case shown, the system is initially well mixed and oscillating red-blue uniformly. The blinking vortex flow is then initiated, and the system is allowed to evolve for over 40 min (about 150 periods of the BZ oscillation) with the blinking vortex flow. Experiments (not shown) are also done in which the blinking vortex flow is not turned on until after a pattern similar to Fig. 3(a) develops. Similar patterns are observed (after a transient period), indicating that the long-term behavior is insensitive to the initial conditions.

The images in Figs. 3(c)–3(e) reveal patterns that reflect the structures seen in the chaotic mixing of passive

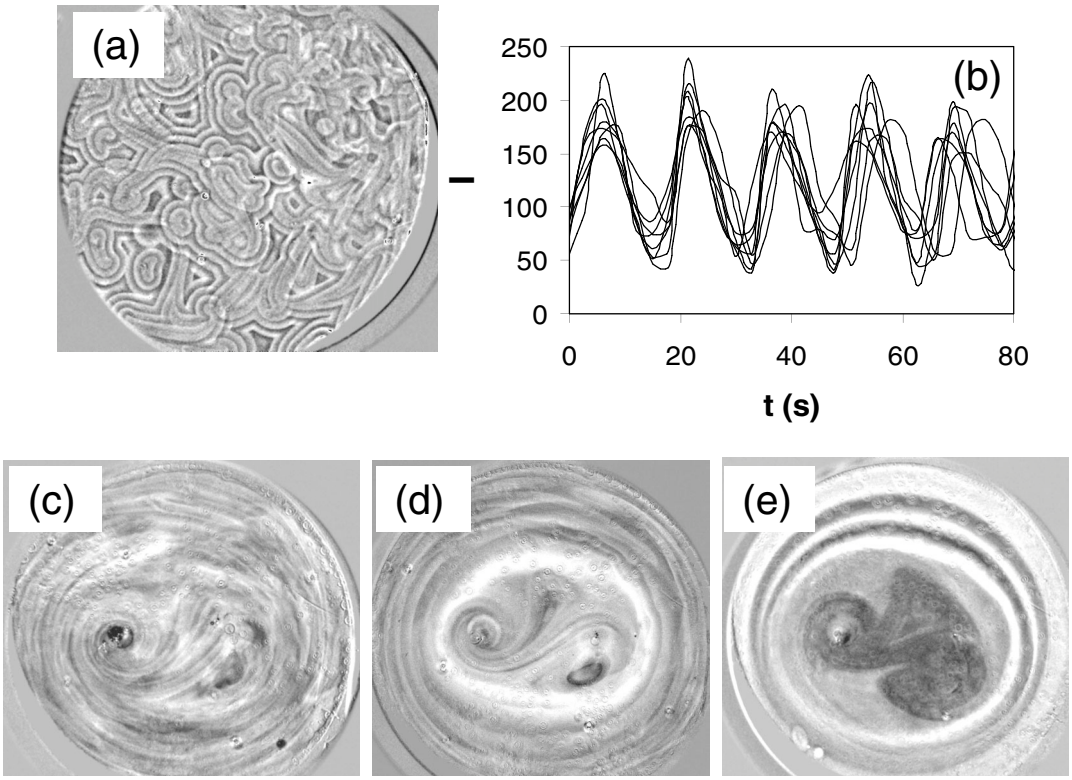

FIG. 3. (a) Patterns for the Belousov-Zhabotinsky reaction in the absence of a driven flow; image taken 29 min after start of run. (b) Time series of intensities (in arbitrary units) taken at the eight different (separated but initially dark) locations in the absence of a flow. (c)–(e) Patterns for the Belousov-Zhabotinsky reaction in the blinking vortex system; $\mu = 0.52$. The blinking frequency f is (c) 0.010, (d) 0.030, and (e) 0.050 Hz. Time after start of run for (c), (d), and (e) is 41, 45, and 46 min, respectively.

impurities with the same value of μ (compare Fig. 3 with Fig. 2), similar to numerical results seen in earlier studies with a blinking vortex-sink flow [21–23]. But there are clear differences as the blinking frequency f and the mixing time τ_m are varied. Given a large τ_m, an intricate pattern forms with variations on small length scales [Fig. 3(c)]. On the other hand, a flow with a small τ_m (but same μ) is characterized by a single, large-scale contiguous pattern that occupies much of the chaotic region in the center [Fig. 3(e)].

The increase in the size of the patterns with decreasing τ_m makes sense; after all, in the limit of perfect mixing ($\tau_m \to 0$), the entire system would oscillate red-blue in unison. The question then is to what time scale τ_m should be compared when considering pattern formation in this system. The typical period of oscillation for the BZ reaction (16 s without a flow and 16–20 s with the flow) is a local time scale, which can depend significantly on the mixing properties of the flow, as shown in previous studies [24]. Furthermore, even in the absence of any advective mixing, distant parts of the system can remain mostly synchronized for several oscillation periods, since all parts of the system oscillate with close to the same frequency. Consequently, a time scale longer than the oscillation period for the BZ reaction is needed.

The time evolution of the BZ pattern found with no flow [Fig. 3(a)] can be used to approximate a characteristic decorrelation time T_{BZ} for pattern formation in the BZ system. Figure 3(b) shows time series of intensities determined at eight different points in Fig. 3(a). The points are chosen such that the oscillations are initially in phase; however, they are widely separated throughout the system (minimum separation of 1.8 cm or about ten wavelengths of the pattern). The large separation assures that there is no diffusive communication between the points during the time scales of the experiment; conse-

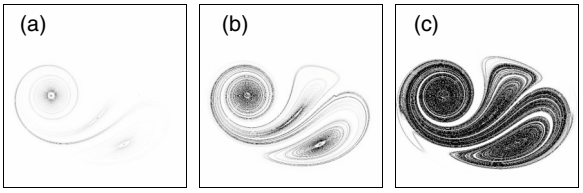

FIG. 4. Simulated maps of the mixing field after (a) 2.0, (b) 3.0, and (c) 5.0 oscillation periods; $\mu = 0.52$. The scaling of the intensity is the same for the three images and has been chosen to highlight the main features. The mixing field for one period of oscillation (not shown), corresponding to $f = 0.010$ Hz, is relatively featureless when plotted with the same scaling factors as those shown here.

quently, the ensuing calculations do not depend on the separation of the points chosen. Since the chosen points do not communicate with each other, the phases of the oscillations drift and the eight points become decorrelated with time. The time series are summed, and the envelope of the combined data is fitted to a decaying exponential to determine a decorrelation time $T_{BZ} \sim 100$ s, more than a factor of 5 longer than the typical BZ oscillation period. The patterns shown in Figs. 3(c)–3(e) are consistent with an assertion that large-scale patterns form if the mixing time τ_m is comparable to or smaller than T_{BZ}.

Insight into the pattern formation process can be found by plotting fields of mixing efficiencies [25]. The trajectories of triplets of tracers (separated initially by $\Delta x_0 = 0.000\,001$ cm) are simulated numerically from Eqs. (1) and (2) on a 600×600 grid. The mixing efficiency ξ at time t is defined by the ratio $\Delta x/\Delta x_0$, where Δx is the largest separation among the triplet at time t. [As defined, ξ is related to the finite-time Lyapunov exponent $\lambda(t)$ via $\lambda(t) = \frac{1}{t} ln(\xi)$.] Regions where ξ is large are those where filaments are stretched most in one direction and thinned most in an orthogonal direction; consequently, these are the regions where advection and diffusion best mix the contents of the fluid.

Fields of the mixing efficiency are shown in Figs. 4(a)–4(c) for two, three, and five periods of oscillation, respectively. These correspond to the number of periods of oscillation equal to the decorrelation time $T_{BZ} \sim 100$ s for blinking frequency $f = 0.020$, 0.030, and 0.050 Hz, respectively. It can be seen that chemical patterns [Figs. 3(d) and 3(e)] form in regions with large mixing efficiencies [dark regions in Figs. 4(b) and 4(c)], although these patterns depend strongly on the mixing time τ_m. The agreement is quite good; even the thin, darkened filaments connecting the two swirls in the reaction patterns for the intermediate case [Fig. 3(d)] are seen in the simulated mixing field [Fig. 4(b)].

These experiments reinforce the recent theoretical and numerical studies [10–13] that indicate that the tools used to describe chaotic mixing can be applied to analyze and predict patterns in a reacting flow. This is evidenced, in particular, by the good correspondence between the simulated mixing fields and the experimental reaction-advection-diffusion patterns in the central chaotic region. Careful consideration, however, needs to be made about the time scales both for the mixing—indicated in this work by τ_m—as well as for the reaction dynamics (T_{BZ}). Behavior similar to that found in these experiments should be expected for a wide variety of reaction-advection-diffusion systems. These include (but are not limited to) phytoplankton blooms in oceanic flows [12,13,26], epidemiological systems, plasmas in fusion reactors, microfluidic processing systems, and cellular processes.

This work was supported by the U.S. National Science Foundation (Grants No. DMR-0071771, No. DMR-0404961, and No. REU-0097424).

*Electronic address: tsolomon@bucknell.edu

[1] P. Grindrod, *The Theory and Applications of Reaction-Diffusion Equations: Patterns and Waves* (Clarendon Press, Oxford, 1996).
[2] D. Ben-Avraham and S. Havlin, *Diffusion and Reactions in Fractals and Disordered Systems* (Cambridge University Press, Cambridge, 2000).
[3] A. T. Winfree, Science **175**, 634 (1972).
[4] K. Showalter, J. Chem. Phys. **73**, 3735 (1980).
[5] R. S. Cantrell, SIAM Rev. **38**, 256 (1996).
[6] D. Vives, J. Armero, A. Marti, L. Ramirez-Piscina, J. Casademunt, J. M. Sancho, and F. Sagues, J. Math. Chem. **23**, 239 (1998).
[7] S. Theodorakis and E. Leontidis, Phys. Rev. E **65**, 026122 (2002).
[8] H. Aref, J. Fluid Mech. **143**, 1 (1984).
[9] J. M. Ottino, *The Kinematics of Mixing: Stretching, Chaos and Transport* (Cambridge University Press, Cambridge, 1989).
[10] Z. Neufeld, Phys. Rev. Lett. **87**, 108301 (2001).
[11] Z. Neufeld, I. Z. Kiss, C. S. Zhou, and J. Kurths, Phys. Rev. Lett. **91**, 084101 (2003).
[12] I. Scheuring, G. Karolyi, T. T. A. Pentek, and Z. Toroczkai, Freshw. Biol. **45**, 123 (2000).
[13] G. Karolyi, A. Pentek, I. Scheuring, T. Tel, and Z. Toroczkai, Proc. Nat. Acad. Sci. U.S.A. **97**, 13 661 (2000).
[14] G. Karolyi, A. Pentek, Z. Toroczkai, T. Tel, and C. Grebogi, Phys. Rev. E **59**, 5468 (1999).
[15] E. Hernandez-Garcia, C. Lopez, and Z. Neufeld, Chaos **12**, 470 (2002).
[16] R. J. Field and M. Burger, *Oscillations and Traveling Waves in Chemical Systems* (Wiley, New York, 1985).
[17] S. K. Scott, *Oscillations, Waves, and Chaos in Chemical Kinetics* (Oxford University Press, Oxford, 1994).
[18] H. Willaime, O. Cardoso, and P. Tabeling, Phys. Rev. E **48**, 288 (1993).
[19] T. H. Solomon, S. Tomas, and J. L. Warner, Phys. Rev. Lett. **77**, 2682 (1996).
[20] T. H. Solomon and I. Mezić, Nature (London) **425**, 376 (2003).
[21] Z. Neufeld, C. Lopez, E. Hernandez-Garcia, and O. Piro, Phys. Rev. E **66**, 066208 (2002).
[22] I. Z. Kiss, J. H. Merkin, and Z. Neufeld, Physica (Amsterdam) **183D**, 175 (2003).
[23] Z. Neufeld and P. Haynes, Chaos **12**, 426 (2002).
[24] C. S. Zhou, J. Kurths, Z. Neufeld, and I. Z. Kiss, Phys. Rev. Lett. **91**, 150601 (2003).
[25] P. D. Swanson and J. M. Ottino, J. Fluid Mech. **213**, 227 (1990).
[26] I. Scheuring, G. Karolyi, Z. Toroczkai, T. Tel, and A. Pentek, Theor. Popul. Biol. **63**, 77 (2003).